Available online at www.sciencedirect.com
ScienceDirect
Polymer 48 (2007) 448–457
polymer
www.elsevier.com/locate/polymer

The effect of solution properties on the morphology of ultrafine electrospun egg albumen–PEO composite fibers

S. Wongsasulak [a], K.M. Kit [b], D.J. McClements [c], T. Yoovidhya [a], J. Weiss [c,*]

[a] Department of Food Engineering, King Mongkut's University of Technology Thonburi, Bangkok 10140, Thailand
[b] Department of Materials Science and Engineering, University of Tennessee, 510 Dougherty Hall, Knoxville, TN 37996, USA
[c] Department of Food Science, University of Massachusetts, Chenoweth Laboratory, 100 Holdsworth Way, Amherst, MA 01003, USA

Received 6 April 2006; received in revised form 30 October 2006; accepted 3 November 2006
Available online 8 December 2006

Abstract

Biocompatible composite fibers suitable for food and medical applications were electrospun from egg albumen (EA) and poly(ethylene oxide) (PEO) at a flow rate of 1.8 mL/min, at an applied voltage of 22 kV and a capillary to target distance of 15 cm. The ratio of EA to PEO dispersed in formic acid was varied from 1:0 to 1:0.1, 1:0.3, 1:0.6 and 0:1. The influence of dispersion properties such as viscosity, surface tension and electrical conductivity on the morphology of electrospun fibers was investigated. As the ratio of PEO increased, viscosity, surface tension, and conductivity decreased. Electrospun fibers had diameters of 188 ± 21, 289 ± 33, 470 ± 32 and 202 ± 20 nm for EA–PEO composite ratios of 1:0.1, 1:0.3, 1:0.6, and 0:1, respectively. Pure EA did not form fibers, but was deposited as beads instead. Results were attributed to increasing entanglement of the two polymers as the concentration of PEO in the solution increased leading to larger diameters of electrospun fibers. Compositional analysis of fibers spun from mixed dispersions using FTIR and TGA indicated that fibers were composed of both EA and PEO, but that fibers contained larger concentrations of PEO than the original dispersions. Investigation of thermal properties by DSC showed the absence of a melting point in 1:0.1 and 1:0.3 EA–PEO fibers. At an EA–PEO ratio of 1:0.6, a melting point characteristic of PEO was identified but enthalpy was significantly smaller than that of pure PEO which could possibly be attributed to molecular interactions between the two polymers.

Keywords: Electrospinning; Egg albumen; Poly(ethylene oxide)

1. Introduction

Interest in the production of fibers from biodegradable and biocompatible synthetic and natural polymers has steadily increased as novel applications within the areas of biomedicine, pharmaceuticals, cosmetics, and food science have emerged. Interest in the food sciences has been driven by the need to develop packaging materials with improved mechanical and barrier properties that are edible and/or biodegradable and the demand for high-performance encapsulation systems. Available biopolymers to create functional matrices include proteins, carbohydrates and (polar) lipids. These materials are often readily available at low cost as byproducts of a food processing operation. Egg albumen (EA) is a highly functional food protein that is frequently used in food matrix design because of its ability to form gel networks, increase solution viscosity, and stabilize emulsions and foams [1]. In previous studies, we focused on the production of solution-cast films from binary mixtures of egg albumen and polysaccharides such as cassava starch [2]. Results of these studies indicated that such matrices were able to entrap lipophilic materials such as essential oils and lipid soluble vitamins to form "active" films that slowly released their content into an adjacent material (e.g., food, skin). However, studies of the microstructure of bi-composite biopolymer films indicated microphase separation due to polymer incompatibility depending on the relative ratio of the two polymers that negatively influenced mechanical properties, long-term stability and release characteristics of solution-cast films.

* Corresponding author. Tel.: +1 413 543 1025; fax: +1 413 543 1262.
E-mail address: jweiss1@foodsci.umass.edu (J. Weiss).

0032-3861/$ - see front matter © 2006 Elsevier Ltd. All rights reserved.
doi:10.1016/j.polymer.2006.11.025

Electrospinning is a technique used to form long nonwoven ultrafine fibers, i.e., fibers with diameters of up to several hundred nanometers [4–6]. In general, fibers may have sizes ranging from 40 to 2000 nm [4,7], but fibers as thick as 5000 nm have been produced [8]. A spun-fiber is produced via ejection of a polymeric jet from a positively charged viscous polymeric solution through a capillary tip to an electrically grounded target. The solvent evaporates rapidly from the ejected jet while it travels the distance from the capillary to the grounded target and solid nanofibers with high surface to volume ratio are deposited on the collector plate. Because of the rapid evaporation and simultaneously superimposed mechanical stresses due to developing bending instabilities of the polymer jet, polymers in electrospun fibers are more oriented than the original polymer and therefore exhibit better mechanical properties and higher thermal stability [9–13]. Consequently, interest in production of electrospun fibers from biodegradable and/or edible biopolymers is gaining increasing interest in the food, pharmaceutical and cosmetics industries. To date, electrospun fibers have been used to manufacture filter media, cosmetic skin masks, nanosensors, military protective clothing, control drug delivery matrices, and tissue scaffolding for wound dressings [6].

The objective of this study was to evaluate the feasibility of producing electrospun fibers from egg albumen–poly(ethylene oxide) composite dispersions and to evaluate the influence of dispersion properties on the morphology of the electrodeposited material. Poly(ethylene oxide) was selected not only because it has previously been shown to produce ultrafine electrospun fibers [7,14], but also because it has properties similar to that of many polysaccharides, i.e., it has a linear structure, water soluble, capable of forming hydrogen bonds with other polymers, and available in a range of different molecular weights. It should be noted that initial experiments using water as a solvent were not successful. Instead, formic acid was used; a solvent which has been noted to be ideal for the production of fibers from polymers containing amine groups (e.g., proteins) [15–18].

2. Materials and methods

2.1. Polymer solution preparation

Egg albumen (EA) powder was obtained from Igreca (Seiches sur le Loir, France). Egg albumen is a commercial product consisting of a mixture of different proteins with molecular weights ranging from 14 to 76 kDa [19]. PEO with an average molecular weight of ~300,000 Da was purchased from Sigma–Aldrich (PA, USA). Polymer dispersions were prepared by dispersing 5 wt% of total polymer at varying mass ratios (1:0, 1:0.1, 1:0.3, 1:0.6 and 0:1) in 95 wt% aqueous formic acid solution (96% formic acid, Sigma–Aldrich, PA, USA). The dispersions were kept at room temperature (25 °C) under constant stirring for at least 1 h prior to the electrospinning experiments to ensure complete dissolution of all polymers in the solvent.

2.2. Electrospinning

An electrospinning apparatus was setup as shown in Fig. 1. A 50-mL syringe (Multifit, Fisher, USA) equipped with a 0.69 mm diameter stainless steel tip (Hamilton No. 91019) was filled with 20 mL of polymer dispersions. The syringe was mounted in a syringe pump (Harvard Apparatus 11P, USA) that allowed the control of the flow rate. The stainless steel tip of the syringe was connected to a high voltage generator (Gamma High Voltage; ES 30P-6W, USA) operated in positive DC mode. A grounded copper plate mounted in a polypropylene block was used as target to collect fibers and/or beads. Preliminary experiments (data not shown) led to the determination of an optimal syringe tip-to-target distance of 15 cm and a flow rate of 0.18 mL/h at an applied voltage of 22 kV. These conditions were kept throughout the experiments. All experiments were carried out at room temperature (25 °C) at a relative humidity of 50 ± 5%.

2.3. Rheology

The apparent viscosity of polymer dispersions was determined by steady-shear rheometry. Shear stress (σ, Pa) of composite polymer dispersions was recorded as a function of

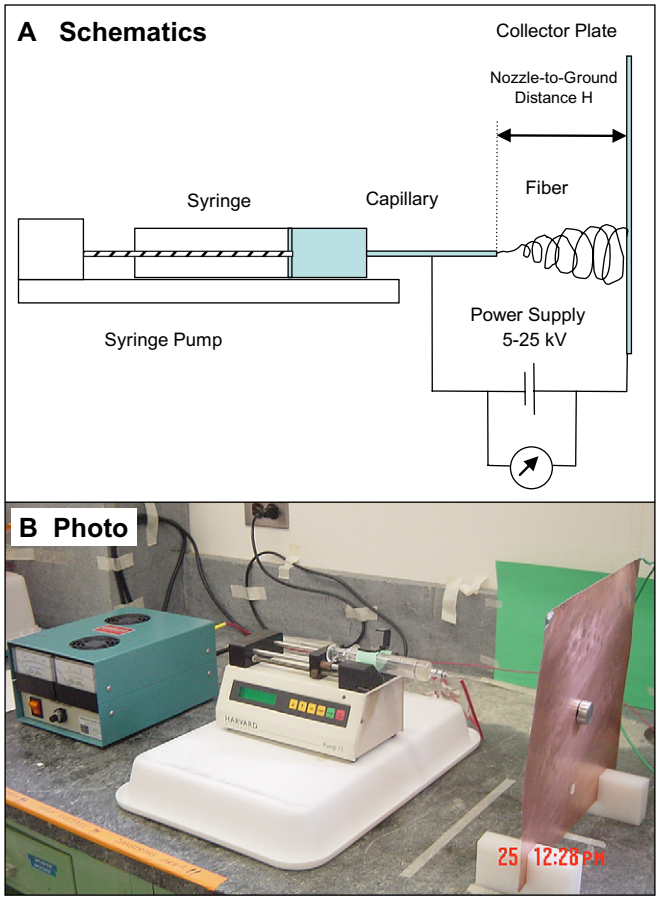

Fig. 1. Setup of the electrospinning apparatus for the production of composite egg albumen–poly(ethylene oxide) fibers.

shear rate ($\dot{\gamma}$, s^{-1}) at controlled shear rates between 10^{-5} and $10^{3}\ s^{-1}$ using a rotational rheometer (MCR 300, Paar Physica, NJ, USA) with a double coaxial bob and cup measurement system (length = 40 mm, diameter = 26.66 mm, gap width = 0.225 mm). The temperature of the loaded sample was equilibrated to 25 °C prior to all measurements using a Peltier system. The reported results are averages from triplicate measurements.

Measurements of shear stress versus strain rate determined by steady-shear rheometry were fitted to the power law model [20]

$$\sigma = K\dot{\gamma}^{n} \quad (1)$$

where σ is the shear stress, $\dot{\gamma}$ is the shear rate, K is the consistency coefficient and n is the flow-behavior index. The flow-behavior index n reflects the viscosity of the solution, i.e., $n = 1$ if the solution behaves Newtonian and $n \neq 1$ if the solution behaves non-Newtonian (e.g., shear thinning or shear thickening).

2.4. Tensiometry

Surface tension of the polymer solutions was determined using a digital tensiometer (Model K 10T, Kruss, Germany) that employs the Wilhelmy plate method. Polymer dispersions of 20 mL were poured into a glass beaker that had been extensively rinsed with dilute chromic acid and double distilled and deionized water to remove any surface-active material. Dispersions were equilibrated to 25 °C and the Wilhelmy plate lowered into the dispersion to form a meniscus. The surface tension (N/m) was calculated from the measured normal forces exerted by the meniscus on the platinum plate. Results represent averages of three measurements using duplicate samples.

2.5. Conductivity

The electrical conductivity of the polymer dispersions was determined using a digital conductivity meter (Model VWR 105, VWR International, PA, USA). Temperature of the dispersions was adjusted prior to the measurements to 25 °C using an oil bath. Results are averages of three measurements using duplicate samples.

2.6. Thermal gravimetric analysis

The change in weight of a 4–6 mg sample of either polymer dispersions or electrodeposited materials as a function of temperature was measured using a thermogravimetric analyzer (TGA-7, Perkin–Elmer, NJ, USA). Samples were heated in platinum pans at a heating rate of 7 °C/min under a nitrogen atmosphere with a flow rate of 50 mL/min. Thermogravimetric data (dm/dT) were recorded from 25 to 700 °C. Data shown represent an average of three scans.

2.7. Differential scanning calorimetry

Thermal analysis of spun fibers was performed using a differential scanning calorimeter (Model Q100 DSC, TA Instruments, DA, USA). Samples weighing 3 ± 0.1 mg were loaded in a DSC pan and the pan was sealed with a crimping tool. Samples were equilibrated to 25 °C for 10 min, and then heated from 25 to 180 °C at a heating rate of 2 °C/min. Curves represent an average of four separate scans.

2.8. Fourier transform infrared spectroscopy

To determine composition and chemical characteristics of fibers, infrared spectra of electrospun fibers were recorded using a Fourier transform infrared spectrophotometer (Model M2000 series, Midac, CA, USA) operating in a wavelength range from 3700 to 650 cm^{-1} with a resolution of 4 cm^{-1}. Each measurement was composed of an average of 16 scans.

2.9. Scanning electron microscopy

The morphology of the electrospun fibers was evaluated by scanning electron microscopy (SEM JSM 5400, JEOL, MA, USA). Fibers were spun directly onto a grounded aluminum SEM stub that was mounted on the collector plate. After deposition of the samples, the stub was sputter coated with Au/Pd in a Polaron E5100 coater at 2 kV, 5 mA for 2 min with an argon backfill at 8 Pa. The average diameter of the electrospun fibers was determined by image analysis (Image J, JEOL, USA) from >200 fibers/sample.

2.10. Statistical analysis

The experiment was designed as a complete randomized block experiment. Results were subjected to statistical analyses using SAS, version 8 (SAS Institute Inc., Cary, NC, USA). Mean separation was achieved using orthogonal polynomial contrast.

3. Results and discussion

3.1. Electrospinning of EA–PEO composites

In this study, EA–PEO bi-composite nanofibers were successfully electrospun using formic acid as solvent. Initially, we investigated the spinnability of EA–PEO mixtures dispersed in water (data not shown). Despite systematic variations of the applied voltage (15–30 kV), tip-to-target distance (5–20 cm), overall polymer concentration (1–16 wt%) and the EA–PEO ratio, no fibers were obtained. At high polymer concentrations, high voltages and medium target-to-tip distances, we observed deposition of particles, but failed to prepare continuous fibers. The shape and size of the electrosprayed microparticles were irregular and non-uniform. Interestingly, however, images obtained from a polarized light microscope revealed highly ordered, possibly crystalline phases in the microparticles. Failure to obtain electrospun fibers from pure

biopolymer dispersions and from mixed polymer–biopolymer dispersions in water has been previously reported [21–23]. It has been speculated that the inability to electrospin pure biopolymer dispersions is due to a lack of entanglement. In addition, dispersion of biopolymers in water or other strongly polar solvents typically leads to the formation of physical gels at even low polymer concentrations that may suppress the formation of a polymer jet [8,24–26].

Initially, dispersion of EA at 1, 3, 5 and 10 wt% protein in formic acid was prepared. Electrosprayed microparticle depositions were imaged under the SEM at protein concentrations of up to 5%. At protein concentrations >5 wt%, EA formed a strong gel that prevented ejection of a polymer jet from the tip of the syringe. Consequently, the maximum (bio)polymer concentration used throughout this study was set at 5 wt%.

Dispersions of EA and PEO in formic acid were prepared and subjected to electrospinning. Fig. 2 shows the scanning electron microscopic images at a magnification of 5000× for EA:PEO dispersion ratios of 1:0, 1:0.1, 1:0.3, 1:0.6 and 0:1. Microparticles were deposited on the collector plate from the pure EA solution. SEM images showed that some of the hairy-beaded structures consisted of dented droplets (Fig. 2a). Similar results have been reported previously and are an indication of low viscosity and low surface tension [16,23,27–29]. Addition of increasing concentrations of PEO (Mw = 300 kDa) to EA resulted in generation of continuous fibers (Fig. 2b–e). EA–PEO composite electrospun fibers were produced at a tip-to-target distance of 15 cm and an applied voltage of 22 kV at a flow rate of 1.8 mL/h (tip diameter ~0.69 mm). Variation of the accelerating voltage (22–27 kV), tip-to-target distance (10–23 cm), and flow rate (1.8–2.4 mL/h) did not significantly affect the morphology of electrospun fibers.

Electrospraying or electrospinning of EA and EA–PEO composite dispersions was initiated when formic acid was used as a solvent instead of water. Formic acid has been noted as a good organic solvent for various polypeptide-based polymers [15–18,30–32]. Moreover, the evaporation rate of formic acid in ambient air (22 °C) has been reported to be 2.3×10^{-8} g/mm^2/s [15]. Compared with water it is therefore significantly more volatile making it an ideal solvent for electrospinning, where rapid evaporation of the solvent after ejection of the polymer jet is desired to prevent the development of discontinuities in the ejected jet [26]. In addition, due to the changes in polymer–polymer and polymer–solvent interactions, the viscosity of polymer solutions in formic acid may substantially differ from that in water [15,16]. Martin et al. [15] for example reported that using formic acid as a solvent for polypeptide-based polymers, the viscosity of the polymeric dispersion increased from 1.6 mPa s to 1–10 Pa s. The rheological behavior of the polymeric dispersion underwent a transition from a simple dispersion behavior to that characteristic for a polymer melt. Leeden et al. [30] attributed this change in the rheological behavior upon dispersion in a 98% formic acid solution to unfolding and swelling of the globular polypeptide structure. They estimated from intrinsic viscosity measurements of β-lactoglobulin in 98% formic acid that the volume of the biopolymer was approximately six times than that in water. The conformational change was further confirmed by CD spectroscopy that suggested a substantial increase in the percentage of random coil structures. It is well known that an increase in the hydrodynamic volume of a polymer in solution is associated with an increase in the degree of polymer entanglement in solution [8]. Therefore, formic acid solutions of EA should have greater entanglement than aqueous solutions, and the formation of fibers via electrospinning will be more favorable.

3.2. Physical properties of composite dispersions and average diameter of electrospun fibers

Distribution of fiber diameters calculated from scanning electron microscopic images using image analysis software indicated that the average fiber diameter increased with increasing concentration of PEO in the bi-component blend (Figs. 2b–e and 3). For example, the average diameter of electrospun EA–PEO fibers increased from 188 ± 22 to 289 ± 33 and 470 ± 32 nm for dispersions containing EA:PEO at ratios of 1:0.1, 1:0.3, 1:0.6, respectively. Pure PEO fibers had an average diameter of 202 ± 20.19 nm. The apparent viscosity of the initial polymer solutions at a shear rate of 100 s^{-1} ($\eta_{a,100}$) increased from 0.015 to 0.039, 0.186, and 0.667 Pa s upon changing the EA:PEO ratios from 1:0 to 1:0.1, 1:0.3, and 1:0.6, respectively (Table 1, Fig. 3). This represents a 2.6, 12.4 and 44.47 times increase over the viscosity of pure EA. The apparent viscosity at 100 s^{-1} of 5 wt% PEO dispersed in formic acid was 1.611 Pa s. Changes in viscosity could be attributed to increased molecular interaction and/or polymer chain entanglement of EA and PEO at increasing PEO concentrations. As was noted by Gupta et al. [8], the morphology of electrospun materials is greatly influenced by polymer viscosity. Varying structures such as microparticles, aggregates of microparticles, fibers containing bead defects and fibers were obtained from the same polymer solution as the polymer concentration in the dispersion was increased. Depending on the polymer concentration, no entanglement was reported for dilute and semi-dilute dispersions, while entanglement was found in the more concentrated solutions that led to the formation of continuous fibers.

Rheological property namely apparent viscosity at the shear rate of 100 s^{-1} with the power law consistency (K) and power law flow-behavior index (n) calculated using Eq. (1) is shown in Table 1. K increased from 0.015 ± 0.001 to 5.69 ± 0.08 Pa s and n decreased from 0.99 ± 0.04 to 0.747 ± 0.003 as the ratio of EA to PEO increased from 1:0 to 0:1. The strong decrease in n with increasing PEO concentrations indicates more pronounced shear thinning behavior which is indicative of increased entanglement. Further evidence of PEO being primarily responsible for the entanglement was obtained from the measurement of the intrinsic viscosity [η] of the two polymers and the determination of the concentration dependence of the viscosity η in the semi-dilute concentration regime. As discussed by Gupta and coauthors [8], the critical chain overlap concentration c^*, that is, the crossover between the

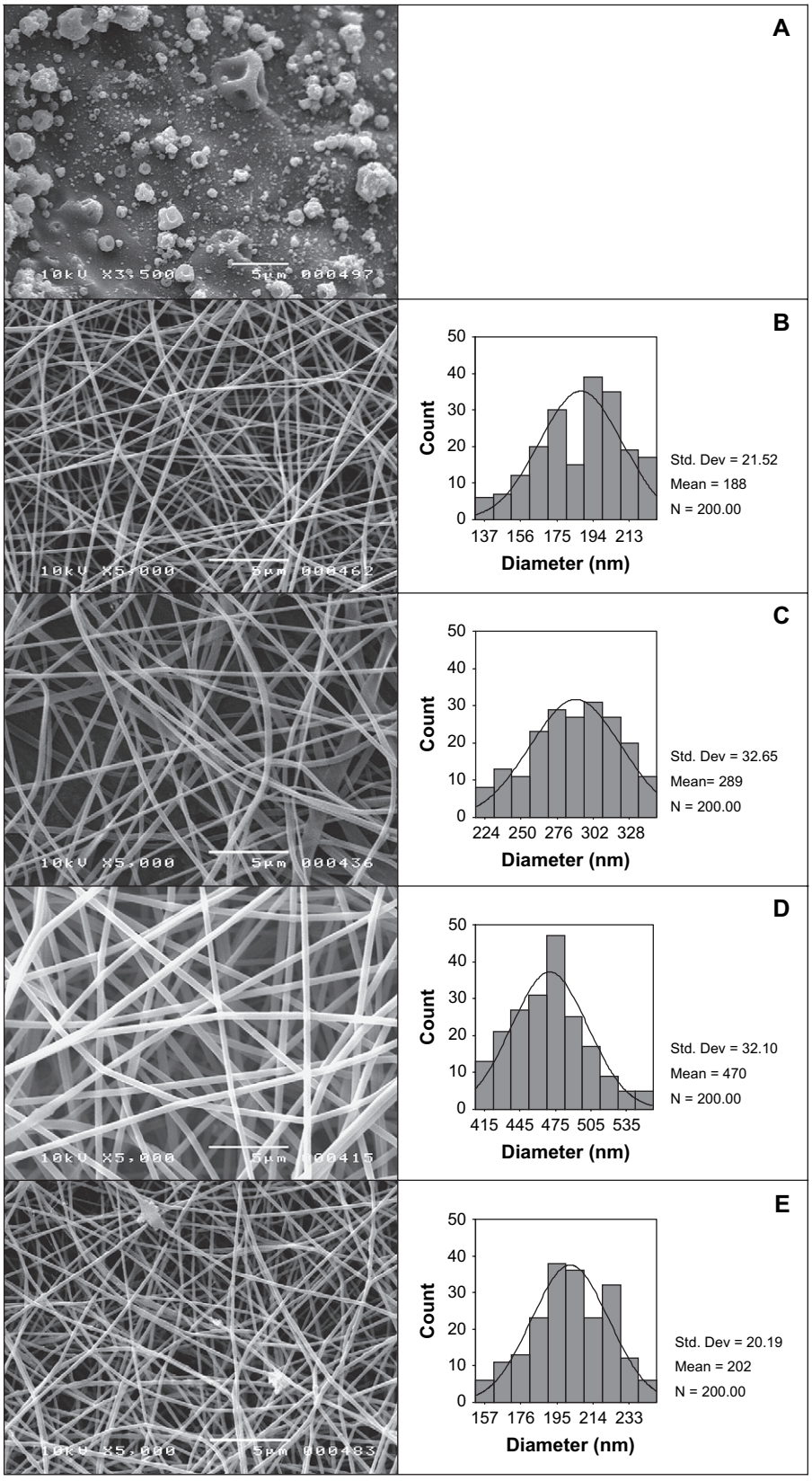

Fig. 2. Scanning electron microscopic images (magnification = 5000×) of depositions of electrospun composite biopolymer dispersions at ratios of EA:PEO of (A) 1:0 (B) 1:0.1 (C) 1:0.3 (D) 1:0.6 (E) 0:1. The total polymer concentration was 5 wt% in formic acid. For fibrous depositions, the distribution of fiber diameters is shown on the right hand side. Electrospinning conditions were $U = 22$ kV, $I = 16.8$ μA, tip-to-target distance = 15 cm, temperature = 25 °C.

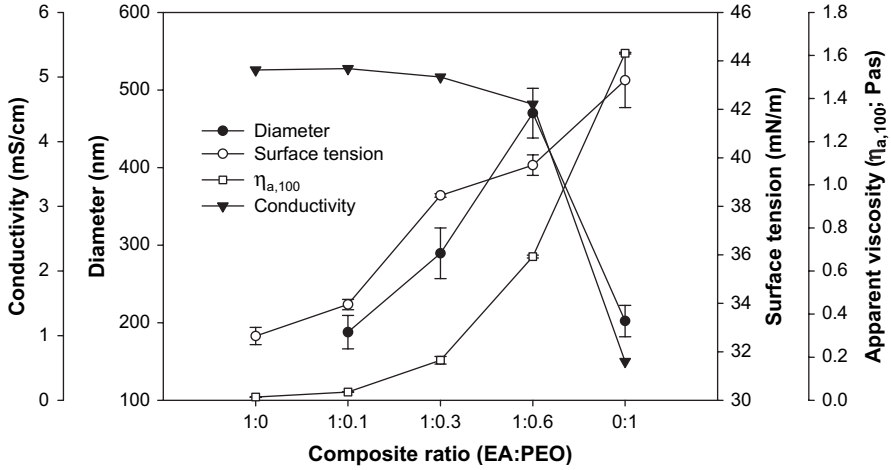

Fig. 3. Viscosity, surface tension, and electrical conductivity of composite egg albumen–poly(ethylene oxide) dispersions as a function of ratio of EA:PEO at a total polymer concentration of 5 wt% in formic acid. The average diameter of electrospun fibers (if fibers were formed) is plotted as a function of the EA:PEO ratio as well.

Table 1
Apparent viscosity at a shear rate of 100 s^{-1}, and power law indices K and n of EA–PEO dispersions as a function of EA:PEO ratio

Composite ratio (EA:PEO)	Apparent viscosity $\eta_{a,100}$ (Pa s)	Power law consistency coefficient (K)	Power law flow-behavior index (n)
1:0	0.014 ± 0.002^{a}	0.015 ± 0.001^{a}	0.989 ± 0.044^{a}
1:0.1	0.039 ± 0.001^{b}	0.044 ± 0.0003^{b}	0.970 ± 0.001^{a}
1:0.3	0.186 ± 0.018^{c}	0.266 ± 0.004^{c}	0.912 ± 0.002^{b}
1:0.6	0.667 ± 0.006^{d}	1.683 ± 0.015^{d}	0.814 ± 0.002^{c}
0:1	1.611 ± 0.004^{e}	5.690 ± 0.082^{e}	0.747 ± 0.003^{d}

The total polymer concentration in formic acid was 5 wt%.
The superscripts a–e indicate statistically significant differences.

dilute and the semi-dilute concentration regimes where the concentration inside a macromolecular chain equals that of the solution concentration, can be estimated as:

$$c^* \sim [\eta]^{-1} \tag{2}$$

The critical chain overlap concentration of PEO and EA was estimated from the intrinsic viscosity as 0.11 and 0.79 g/dL. Measurement of the viscosity of a series of solutions of the PEO and EA above their respective c^* up to the polymer concentration used in this study and subsequent fit to a power law model showed that $\eta \sim c^{4.08}$ and $\eta \sim c^{1.32}$ for PEO and EA, respectively. The weaker concentration dependence of the EA solution is typical for unentangled polymers in the semi-dilute concentration regime. For example, concentration exponents between 1.1 and 1.4 have been reported for semi-dilute unentangled solutions of polymers [8]. In contrast, exponents of 4.25–4.5 are typical for semi-dilute entangled polymer solutions suggesting that the PEO polymers were likely entangled in the solution used for the electrospinning experiments.

The surface tension and electrical conductivity of the 5 wt% EA dispersion in formic acid at 25 °C were 32.7 mN/m and 5.12 mS/cm, respectively (Fig. 3). Surface tension increased from 32.7 to 33.9, 38.5, 39.7 and 43.2 mN/m as the PEO concentration in the composite dispersion increased from 1:0 to 0:1. The contribution of the dissolved polymer to the overall surface tension is typically small unless the polymer has amphiphilic properties [6]. However, EA as a protein is a surface-active molecule that has the tendency to adsorb at interfaces and undergo structural rearrangement (surface denaturation). The surface tension of formic acid therefore decreased upon addition of EA from 38.5 to 32.7 mN/m. The increase in surface tension with increasing PEO concentration may be attributed to a change in the interfacial composition of the polymer dispersion. The electrical conductivity of polymer dispersions simultaneously decreased to 5.1, 5.0, 4.6 and 0.6 as the PEO ratio increased from 1:0 to 1:0.1, 1:0.3, 1:0.6 and 0:1. Formation of a fluid jet generally depends on sufficiently high surface charge densities that are influenced not only by the applied voltage but also by the conductivity of the polymer dispersion [33]. Differences in conductivities of composite EA–PEO polymer dispersions were relatively small and do not explain the observed large changes in fiber diameter (Fig. 3). However, it has been noted that surface morphology of fibers (e.g., smoothness) may increase as the conductivity increased, but additional experiments using atomic force microscopy or field emission scanning electron microscopy may be needed to verify whether this was the case here.

As has been noted by several authors, the physicochemical properties of polymer dispersions such as viscosity, surface tension and conductivity play a key role in the formation of continuous fibers [7,8,16,23,24,26–29]. Generally, polymer filaments are formed between two electrodes that are oppositely charged, because application of the high voltage electric field induces a charge in the surface of the liquid inside the capillary tube used to eject the polymer dispersion. The electrostatic repulsion on the surface of the fluid increases with increasing electric field strength. In the process, the hemispherical surface of the fluid at the tip of the capillary is elongationally distorted to create the characteristic Taylor cone [4].

Eventually, the molecular interaction forces have to become large enough to overcome the opposing surface tension in order for a charged polymer fluid jet to be ejected from the tip of the Taylor cone [4,27,34,35]. Thus lower surface tensions (e.g., through addition of surfactants) may help overcome electrospinning opposing forces. Water with a very high interfacial tension (72 mN/m) is therefore a particularly poor solvent for electrospinning. Moreover, to form a continuous fiber, polymers need to be sufficiently entangled. Otherwise, microparticles or beads are deposited instead of fibers. Upon ejection of the charged solution from the small-diameter spinneret, the solvent rapidly evaporates forming the solid fibers that are deposited on the collector [6]. As previously discussed, rheology of EA–PEO dispersions indicates that the degree of entanglement increases as PEO is added, which likely is one of the key factors that explains the production of composite fibers.

3.3. Compositional analysis of electrospun fibers by Fourier transform infrared spectroscopy (FTIR) and differential thermal gravimetry (DTG)

Infrared absorption spectra of composite EA–PEO fibers indicated that electrospun fibers were composed of both EA and PEO (Fig. 4). Characteristic peaks for pure PEO fibers were identified at ~2900, 1100 and 958 cm^{-1}. The absorption peak at 2900 cm^{-1} can be attributed to the molecular stretching of the methylene group (CH_2) while peaks at 1100 and 958 cm^{-1} are due to stretching of the C–O–C group in PEO [23,36–38]. FTIR spectra of pure powdered EA showed characteristic peaks at ~3360, 2950, 2858 and 1650 cm^{-1} typical for amides and amines, major functional groups of many proteins [39]. Deconvolution of FTIR spectra using single component spectra (pure EA and pure PEO) and subsequent calculation of peak areas are shown in Fig. 5. FTIR spectra also indicate the formation of new groups possibly due to molecular interactions between EA and PEO.

Differential thermogravimetric analysis of weight loss of samples as a function of oven temperature is shown in Fig. 6. Change in weight of electrodeposited samples with temperature confirmed that fibers were composed of both polymers. Thermal degradation of pure PEO electrospun fibers was observed at ~380 °C while pure EA electrosprayed deposits degraded over a temperature range of 190–275 °C. Composite fibers had characteristic weight losses at both 190–275 and 380 °C. Deconvolution of the differential thermal degradation spectra shown in Fig. 6 followed by the integration of the peak areas was used to calculate the absolute composition of fibers (Fig. 7). Significant deviations in concentration of PEO in composite fibers compared to that of polymer dispersions were found, that is, fibers were generally composed of higher concentrations of PEO than in corresponding solutions. For example, EA–PEO fibers produced from 1:0.1 dispersions contained 26.49% PEO suggesting that PEO is preferentially ejected from the polymer dispersion surface.

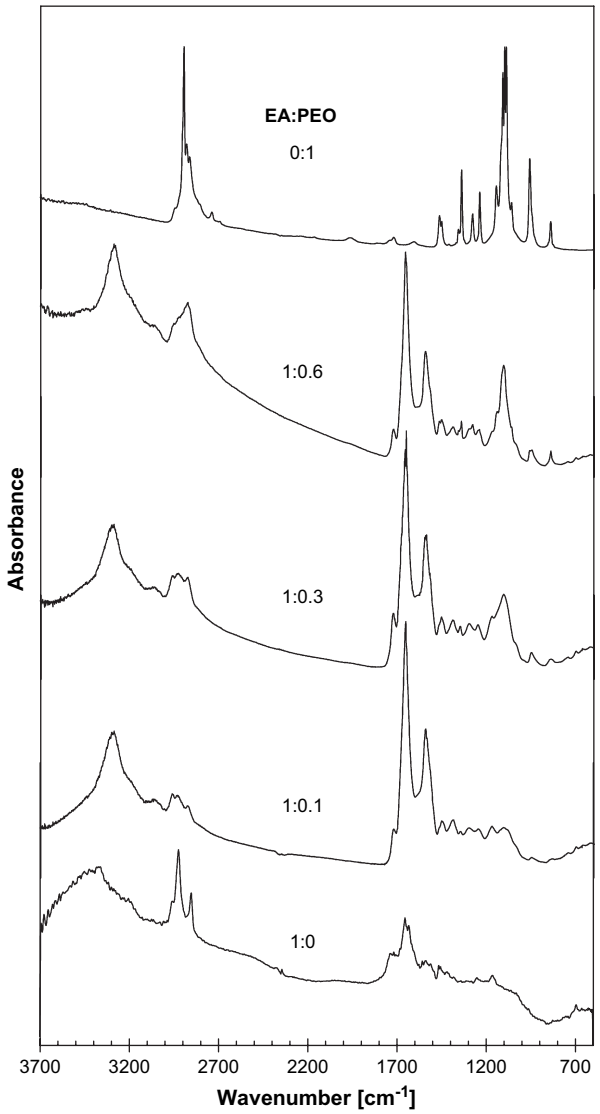

Fig. 4. Infrared absorbance spectra of electrospun EA–PEO fibers (or depositions) at EA:PEO ratios of 1:0, 1:0.1, 1:0.3, 1:0.6 and 0:1 at wave numbers ranging from 3700 to 650 cm^{-1}.

3.4. Thermal properties of electrospun fibers

Finally, the heat flow of electrodepositions as a function of temperature at varying ratios of EA to PEO was measured by DSC (Fig. 8). During the initial heating from 20 to 180 °C at a scanning speed of 2 °C/min, melting of PEO was observed in pure PEO and 1:0.6 composite fibers, but no transition was found in 1:0.1 and 1:0.3 fibers. The melting temperature (T_m) of PEO in the composite sample increased from 57.7 ± 0.2 to 60.6 ± 0.1 °C compared to the pure PEO electrospun fiber. Cooling of samples to 20 °C indicated a peak at ~32 °C for the pure PEO and the 1:0.6 and 1:0.3 samples which may be attributed to a recrystallization of PEO in the matrix. Upon a second heating, a melting of PEO was observed in all the samples containing PEO, but the transition temperatures were higher than that of pure PEO electrospun fibers. The DSC data of all EA containing depositions indicated a phase transition at around 160 °C which could

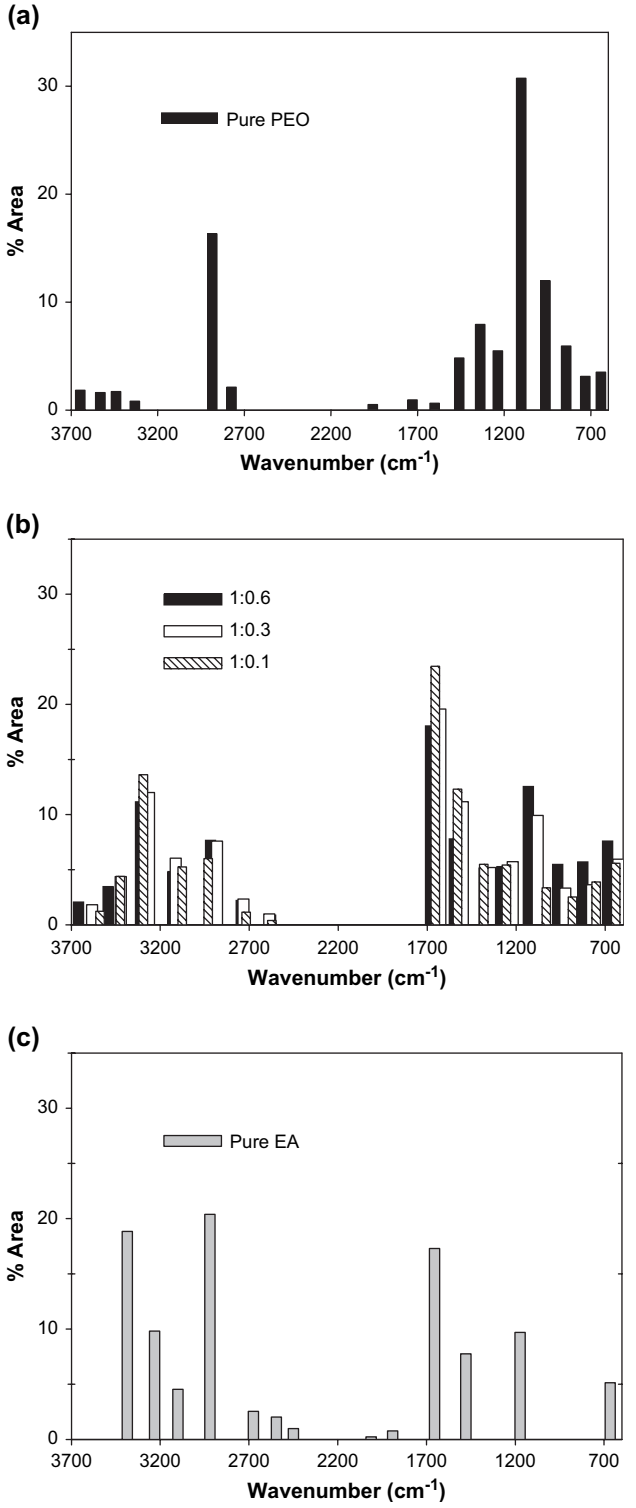

Fig. 5. Integrated peak areas of FTIR spectra of: (a) pure PEO depositions (fibers), (b) EA–PEO depositions (fibers) at composite ratios of 1:0.1, 1:0.3, 1:0.6 and (c) pure egg albumen depositions (beads).

be attributed to egg albumen. While the transition temperature was independent of the egg albumen content, the enthalpy of the transitions decreased as the mass fraction of egg albumen in the composite decreased. Interestingly, a comparison of electrospun fibers and solution-cast EA–PEO films revealed

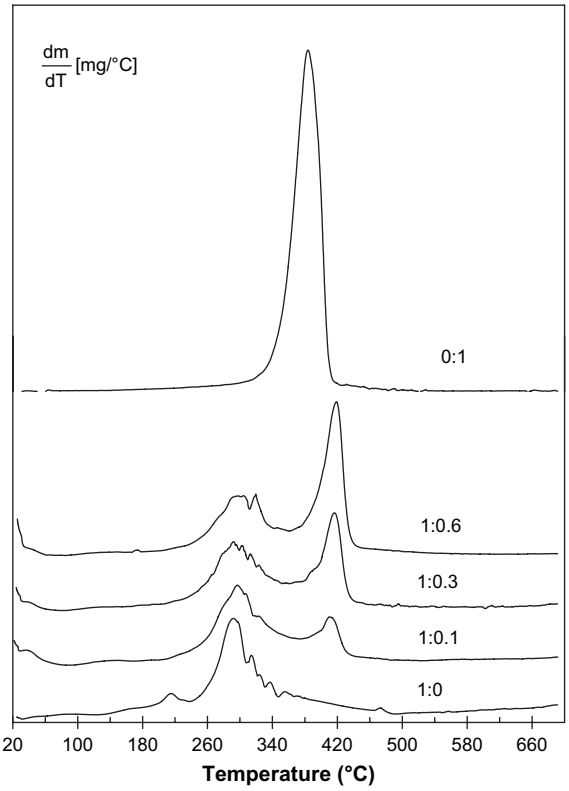

Fig. 6. Derivative thermogravimetric curve dm/dT in mg/°C as a function of oven temperature T for electrospun depositions from 5 wt% composite biopolymer dispersions at EA:PEO ratios of 1:0, 1:0.1, 1:0.3, 1:0.6 and 0:1.

that both transition enthalpy and temperature of structures fabricated by electrospinning were substantially higher than those measured in cast-film [2,9]. This indicates that electrospinning may yield structures of a higher order compared to traditional solution-cast materials leading to improved thermal stabilities, a fact that is of particular importance in food, pharmaceutical and medical applications.

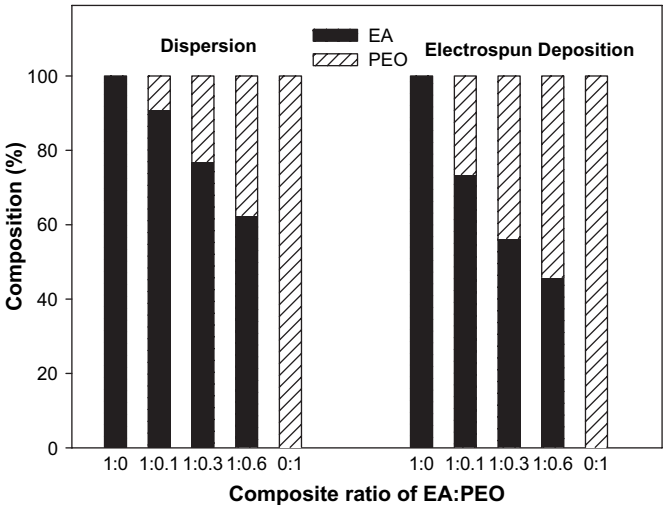

Fig. 7. Comparison of composition of egg albumen–poly(ethylene oxide) dispersion and electrospun deposition fibers at EA:PEO ratio of 1:0, 1:0.1, 1:0.3, 1:0.6 calculated from the thermogravimetric analysis shown in Fig. 6.

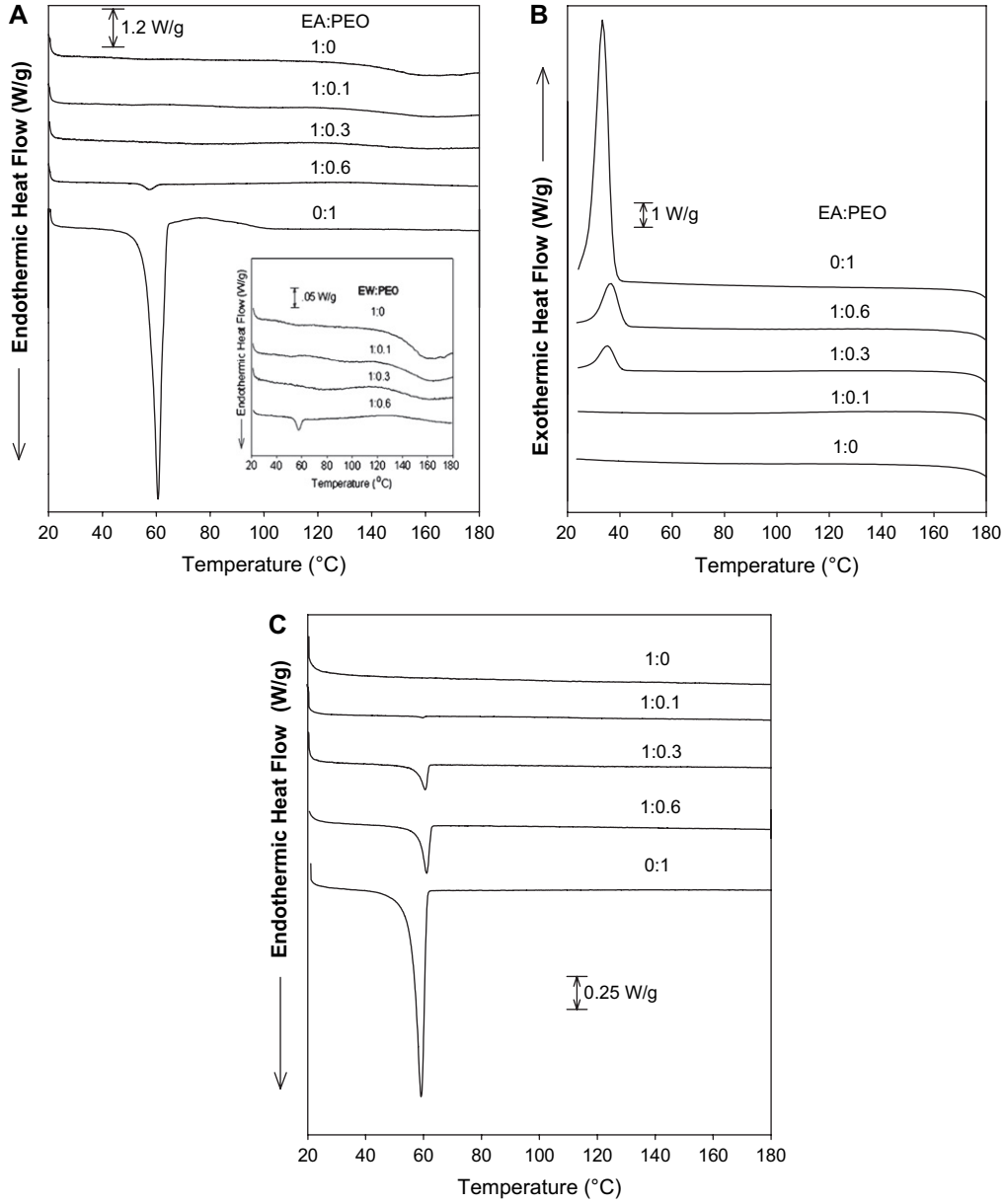

Fig. 8. Heat flow of EA–PEO composite electrospun fibers (EA:PEO ratios of 1:0, 1:0.1, 1:0.3, 1:0.6 and 0:1) measured at a scanning speed of 2 °C/min. (A) Initial heating from 20 to 180 °C, (B) cooling from 180 to 20 °C, (C) secondary heating from 20 to 180 °C.

4. Conclusions

Electrospun fibers were obtained from EA–PEO composite dispersions in formic acid. Electrospinning of pure egg albumen was not successful but led to the deposition of microparticles on the collector plate. Measurement of dispersion properties including viscosity, electrical conductivity and surface tension suggests that egg albumen lacks sufficient entanglement to produce continuous fibers. We base this suggestion on the addition of PEO to the dispersion results in increased entanglement as manifested in the increase in solution viscosity which results in the ejection of a continuous polymer jet that consists of both polymers. However, increased concentrations of PEO seem to be present in the jet suggesting that egg albumen is carried as a minor part of the entangled PEO network. Our study verified that novel biocompatible composite electrospun fibers can be manufactured from EA and PEO and that morphology of fibers is strongly influenced by the dispersion composition. Additional studies should be carried out that elucidate further on the spatial distribution of egg albumen and PEO in the solid fiber to determine whether microphase separations of preferential accumulation of EA at the surface of fibers occurred.

Acknowledgements

This work was supported by a grant from the Thailand Research Fund (TRF) through The Royal Golden Jubilee Ph.D. Program (Grant number; PHD/0284/2545), the Environmental Protection Agency Star Grant Program (Grant number:

GR832372) and the Massachusetts Experiment Station supported by the Cooperative State Research, Extension, Education Service, United State Department of Agriculture, Massachusetts Agricultural Experiment Station (Projects No. 831 and 911). The authors would like to thank D.A. Callaham for his help in the SEM image preparation. Dried EA powder was donated by Igreca, France.

References

[1] Kinsella JE. Relationship between structure and functional properties of food protein. In: Fox PF, Condon JJ, editors. Food protein. London: Applied Science; 1985. p. 51–103.
[2] Wongsasulak S, Yoovidhya T, Bhumiratana S, Hongsprabhas P, McClements DJ, Weiss J. Food Res Int 2006;39:277–84.
[4] Reneker DH, Chun I. Nanotechnology 1996;7:216–23.
[5] Huang ZM, Zhang YZ, Kotaki M, Ramakrishna S. Compos Sci Technol 2003;63:2223–53.
[6] Xu X, Yang L, Xu X, Wang X, Chen X, Liang Q, et al. J Controlled Release 2005;108:33–42.
[7] Son WK, Youk JH, Lee TS, Park WH. Polymer 2004;45:2959–66.
[8] Gupta P, Elkins C, Long TE, Wilkes GL. Polymer 2005;46:4799–810.
[9] Wongsasulak S. Release mechanisms of paprika oleoresin from composite structure of egg albumen and cassava starch. PhD thesis, University of King Mongkut's University of Technology Thonburi, Thailand; 2005.
[10] Zhang YZ, Venugopal J, Huang ZM, Lim CT, Ramakrishna S. Polymer 2006;47:2911–7.
[11] Bognitzki M, Czado W, Frese T, Schaper A, Hellwig M, Steinhart M, et al. Adv Mater 2001;13:70–2.
[12] Shao C, Kim HY, Gong J, Ding B, Lee DR, Park SJ. Mater Lett 2003;57:1579–84.
[13] Huang L, McMillan RA, Apkarian B, Pourdeyhimi EL, Conticello VP, Chaikof EL. Macromolecules 2000;33:2989–97.
[14] Theron SA, Zussman E, Yarin AL. Polymer 2004;45:2017–30.
[15] Martin DC, Jiang T, Buchko J. Protein-based materials. Boston: Birkhauser; 1997.
[16] Bucho CJ, Chen LC, Shen Y, Martin DC. Polymer 1999;40:7397–407.
[17] Park WH, Jeong L, Yoo D, Hudson S. Polymer 2004;45:7151–7.
[18] Ki CH, Beak DH, Gang KD, Lee KH, Um IC, Park YH. Polymer 2005;46:5094–102.
[19] Li-Chan EC, Powrie WD, Nakai S. The chemistry of eggs and egg products. In: Stadelman WJ, Cotterill OJ, editors. Egg science and technology. 4th ed. New York: Food Product Press; 1995. p. 105–75.
[20] Lapasin R, Pricl S. Secondary and tertiary structure of polysaccharides in solutions and gels: rheology of industrial polysaccharides – theory and applications. Melbourne: Blackie Academic and Professional Publishers; 1995.
[21] Huang L, Nagapudi K, Apkarian R, Chaikof EL. J Biomater Sci Polym Ed 2001;2:974–94.
[22] Rho KS, Jeong L, Lee G, Seo BM, Park YJ, Hong SD, et al. Biomaterials 2006;27:1452–61.
[23] Duan B, Dong C, Yuan X, Yao K. J Biomater Sci Polym Ed 2004;15:797–811.
[24] Geng X, Kwon OH, Jang J. Biomaterials 2005;26:5427–32.
[25] Huang ZM, Zhang YZ, Ramakrishna S, Lim CT. Polymer 2004;45:5361–8.
[26] Shenoy SL, Frisch HL, Bates WD, Wnek GE. Polymer 2005;46:3372–84.
[27] Dietzel JM, Beck Tan NC, Kleinmeyer JD, Rehrmann J, Tevault D, Reneker D, et al. Army research laboratory technical report; 1989–1999.
[28] Zong X, Kim K, Fang D, Ran S, Hsiao B, Chu B. Polymer 2002;43:4403–12.
[29] McKee MG, Elkins CL, Long TE. Polymer 2004;45:8705–15.
[30] Leeden VDMC, Rutten AACM, Frens G. J Biotechnol 2000;79:211–21.
[31] Um IC, Kweon HY, Park YH, Hudson S. Int J Biol Macromol 2001;33:91–7.
[32] George L, Sander W. Spectrochim Acta Part A 2004;60:3225–32.
[33] Reneker DH, Yarin AL, Fong H, Koombhongse S. J Appl Phys 2000;87:4531–47.
[34] Michelson D. Electrostatic atomization. Bristol: Adam Hilger; 1990.
[35] Yarin AL, Koombhongse S, Reneker DH. J Appl Phys 2001;90:4836–46.
[36] Jackson M, Haris PI, Chapman D. J Mol Struct 1989;214:329–55.
[37] Ingle Jr JD, Crouch SR. Spectrochemical analysis. New Jersey, Englewood Cliffs: Prentice Hall; 1988.
[38] Ngarize S, Adams A, Howell NK. Food Hydrocolloids 2004;18:49–59.
[39] Creighton TE. Proteins structures and molecular properties. New York: WH Freeman and Company; 1993.